Deviation from tidal symmetry for scattering of polarized ^{23}Na from the deformed nucleus ^{27}Al

N. J. Davis*
School of Sciences, Staffordshire University, College Road, Stoke-on-Trent ST4 2DE, England
and Department of Physics and Astronomy, University of Edinburgh, Mayfield Road, Edinburgh EH9 3JZ, Scotland

H. D. Choi†
Department of Nuclear Engineering, Seoul National University, Seoul 151-742, Korea
and School of Physics and Astronomy, University of Birmingham, Edgbaston, Birmingham B15 2TT, England

R. P. Ward*
School of Sciences, Staffordshire University, College Road, Stoke-on-Trent ST4 2DE, England
and School of Physics and Astronomy, University of Birmingham, Edgbaston, Birmingham B15 2TT, England

P. J. Woods, D. G. Ireland,‡ K. Livingston,‡ R. D. Page,§ P. J. Sellin,‖ and A. C. Shotter
Department of Physics and Astronomy, University of Edinburgh, Mayfield Road, Edinburgh EH9 3JZ, Scotland

J. A. R. Griffith, S. J. Hall, P. R. Dee, I. Martel-Bravo,¶ J. M. Nelson, and K. Rusek**
School of Physics and Astronomy, University of Birmingham, Edgbaston, Birmingham B15 2TT, England
(Received 30 March 1999; published 27 July 1999)

The second-rank analyzing powers T_{20} and $^{T}T_{20}$ were measured using a tensor-polarized beam of ^{23}Na scattered from ^{27}Al at an incident energy of 150 MeV. The concept of tidal symmetry in scattering systems leads directly to a shape-effect relationship between the two sets of analyzing powers which should hold good at low values of the isocentrifugal parameter and this has been confirmed in other scattering systems. For ^{23}Na+ ^{27}Al at 150 MeV the isocentrifugal parameter has the low value of 0.04, yet the shape effect relations do not hold true for the data forward of 12° c.m. It is suggested that this may be evidence for an effect of the deformation of the target nucleus and this is supported by coupled-channel calculations which agree well with the data. [S0556-2813(99)07108-3]

PACS number(s): 24.70.+s, 25.70.Bc, 27.30.+t, 24.10.Eq

I. INTRODUCTION

The concept of tidal symmetry has provided an advance in the understanding of heavy ion collisions over recent years. Tidal symmetry [1] is a dynamical symmetry of the interaction between nuclei. If the forces between the nuclei are central, they are known as tidal forces, from analogy with the gravitational forces between Moon and Earth which create the tides. For such forces the total potential energy of the interaction between the nuclei is clearly invariant under rotations about the line joining their centers. The generator of such rotations is known as the tidal-spin operator and has eigenvalues which are the tidal spin [2], which is conserved under tidal forces. The concept of tidal spin is meaningful provided there is no significant mass exchange between the nuclei on collision, and so it is particularly applicable to elastic scattering.

It is well known that the second-rank analyzing powers for Fresnel scattering systems are related to each other by the shape-effect relations [3]. It has also been shown [2] that tidal symmetry leads directly to the shape-effect relations. The shape-effect relations consequently provide a signature for tidal symmetry and any deviation of the measured analyzing powers from the shape-effect relations indicates that tidal symmetry cannot be applied in the scattering. The shape-effect relation which relates the T_{20} and $^{T}T_{20}$ analyzing powers is

$$T_{20}=\frac{(3\cos\theta-1)^{T}T_{20}}{2}, \tag{1}$$

where θ is the center-of-mass scattering angle. The analyzing power $^{T}T_{20}$ is measured as for T_{20} except that the quantization axis for the beam polarization is taken in the transverse direction [4], normal to the scattering plane, rather than in the beam direction. Because it is related to both T_{20} and T_{22} by

*Present address: School of Sciences, Staffordshire University, College Road, Stoke-on-Trent ST4 2DE, UK.
†Present address: Department of Nuclear Engineering, Seoul National University, Seoul 151-742, Korea.
‡Present address: Department of Physics and Astronomy, University of Glasgow, Glasgow G12 8QQ, UK.
§Present address: University of Liverpool, Oliver Lodge Laboratory, Oxford Street, Liverpool L69 7ZE, UK.
‖Present address: Department of Physics, University of Surrey, Guildford GU2 5XH, UK.
¶Present address: Departmento de FAMN, Facultad de Fisicas, Universidad de Sevilla, Aptdo. 1065, E-41080 Sevilla, Spain.
**Present address: Department of Nuclear Reactions, The A. Soltan Institute for Nuclear Studies, Hoza 69, PL-00681 Warsaw, Poland.

$$^{T}T_{20}=\frac{-(T_{20}+\sqrt{6}T_{22})}{2}, \tag{2}$$

it constitutes a convenient, independent experimental quantity. In the current work, angular distributions of T_{20} and $^{T}T_{20}$ analyzing powers were measured for 150-MeV elastic scattering of ^{23}Na from ^{27}Al, in order to investigate how well they conform to the above relation and if any deviation from tidal symmetry is observed.

The complete Hamiltonian describing the colliding nuclear system depends not only on the central interaction potential but also on the centrifugal term $\mathbf{L}^2/r^2$, for angular momentum operator $\mathbf{L}$ and distance between nuclei r, which can change the tidal spin by ± 1. The centrifugal term may be approximated by setting $\mathbf{L}^2=L(L+1)$ where L is the average of the incoming and outgoing angular momenta. This is known as the isocentrifugal approximation and tidal symmetry holds if this approximation is good [5]. A determination of the validity of the isocentrifugal approximation can be made by defining an isocentrifugal parameter [5]

$$d=\left|1-\frac{f_L^2}{f_{L+1}f_{L-1}}\right|, \tag{3}$$

where f_L is the wave function distorted by the central potential, for a grazing value of L. This is a function of r but calculated at the strong-absorption radius. The isocentrifugal parameter for any given system of colliding nuclei at a given beam energy may be determined from the Sommerfeld parameter at the Coulomb barrier and the scattering energy. The isocentrifugal parameter is small if the isocentrifugal approximation is good and hence tidal symmetry is expected to hold for small isocentrifugal parameters regardless of whether the scattering system is of Fresnel or Fraunhofer type. This has been verified experimentally using spherical target nuclei where tidal symmetry has been found to hold for elastic scattering of ^{7}Li [6–8] and ^{23}Na [9–11] projectiles.

Since scattering systems involving spherical target nuclei are special cases within the realm of all nuclei, it is important to investigate the validity of tidal symmetry for deformed target nuclei. Nuclear scattering in general may be well described by Fraunhofer or Fresnel diffraction descriptions, of which heavy-ion scattering systems constitute predominantly the Fresnel type [12]. Nuclear deformation has, however, been found [13] to cause a deviation of the differential cross section from the Fresnel shape. Therefore it seems possible that target nucleus deformation may also give rise to deviations from tidal symmetry in heavy-ion collisions because the interaction potential may be altered. In an interaction with a deformed target nucleus, different partial waves are more likely to be involved in entrance and exit channels, thus reducing the extent to which the isocentrifugal approximation is valid and hence whether tidal symmetry can be successfully applied.

The aim of the current work is to investigate if there is any deviation from tidal symmetry for scattering from a deformed target nucleus. In order to do this it is necessary to select a scattering system which would otherwise be expected to conform to tidal symmetry, a heavy-ion system with a small isocentrifugal parameter. To achieve this a ^{23}Na beam at 150 MeV and an ^{27}Al target were chosen which provides a suitable deformed nucleus with the ground-state (g.s.) well resolved from the first-excited state at 0.84 MeV. The 150-MeV beam energy gives a value of the isocentrifugal parameter as defined by Ott *et al.* [5] close to 0.04, which is smaller than the value 0.07 for either the ^{7}Li+^{120}Sn system at 44 MeV [7] or the ^{7}Li+^{54}Fe system at 70 MeV [8], while it is larger than the value <0.01 for the ^{23}Na+^{208}Pb system at 170 MeV [9,11]. In these systems with small isocentrifugal parameters, tidal symmetry was found to hold good.

TABLE I. Optical-potential parameters used in the calculations. r_0 and a are the reduced radius and diffuseness parameters, respectively.

V (MeV)	W (MeV)	r_0 (fm)	a (fm)	r_C (fm)
130.0	48.76	1.203	0.50	1.32

II. COUPLED-CHANNEL CALCULATIONS

The calculations were performed using the computer code FRESCO [14]. The optical potential is a Woods-Saxon shape with the same geometry for the real (V) and imaginary (W) parts and is listed in Table I. The central part of the nuclear potential is taken from a fit to a similar elastic scattering system ^{32}S+^{27}Al [15], with a slight modification of the real strength and the reduced Coulomb radius parameter r_C.

The coupling potentials are based on the quadrupole-deformed potentials of the nuclear and Coulomb couplings, of which the nuclear coupling form factor is given by

$$F(r)=-\frac{1}{\sqrt{4\pi}}\delta_2\frac{dU}{dr}, \tag{4}$$

where δ_2 is the nuclear quadrupole deformation length and U is the central nuclear potential. The Coulomb form factor for a large radius is given by

$$F(r)=M(E2)\frac{\sqrt{4\pi}Ze^2}{5r^3}, \tag{5}$$

where $M(E2)$ is the reduced matrix element for the Coulomb transition and Z is the atomic number. The coupling potentials for projectile and target nuclei are produced by simply assuming both nuclei are pure rotational nuclei with band spin equal to the spin of the ground state, whence the nuclear deformation length and the reduced matrix element can be given in terms of the intrinsic quadrupole moment which can be obtained from the experimental spectroscopic quadrupole moment.

For both nuclei, a comparison of the experimental $B(E2)$ values and the spectroscopic quadrupole moments (Q_s) of excited states with those values calculated using the experimental g.s. quadrupole moment and rotational model expres-

TABLE II. A comparison of experimental (Expt.) spectroscopic quadrupole moments of ground and excited states and $B(E2)$ values from references, with values calculated from the g.s. quadrupole moment in the rotational model (Rot. model) with band spin $K=I_{\text{g.s.}}$.

^{23}Na		Q_s (e fm^2)			$B(E2)$	(e^2 fm^4)	
I^π	E_{ex} (MeV)	Expt.	Rot. model	I_i	I_f	Expt. [a]	Rot. model
$\frac{3}{2}^+$	0.0	10.06 ± 0.20 [a]	10.06 ± 0.20 [a]	$\frac{3}{2}^+$	$\frac{5}{2}^+$	143 ± 9	129 ± 5
$\frac{5}{2}^+$	0.440	-5 ± 5 [b]	-3.6 ± 0.1	$\frac{3}{2}^+$	$\frac{7}{2}^+$	73 ± 10	72 ± 3
$\frac{7}{2}^+$	2.076	-14 ± 14 [b]	-10.1 ± 0.2	$\frac{5}{2}^+$	$\frac{7}{2}^+$	60 ± 21	90 ± 4
^{27}Al		Q_s (e fm^2)			$B(E2)$	(e^2 fm^4)	
I^π	E_{ex} (MeV)	Expt.	Rot. model	I_i	I_f	Expt. [c]	Rot. model
$\frac{5}{2}^+$	0.0	14.02 ± 0.10 [d]	14.02 ± 0.10 [d]	$\frac{5}{2}^+$	$\frac{7}{2}^+$	71 ± 19 [e]	73 ± 1.0
$\frac{7}{2}^+$	2.211	0 ± 3 [f]	2.62 ± 0.02	$\frac{5}{2}^+$	$\frac{9}{2}^+$	59 ± 6	26 ± 0.4
$\frac{9}{2}^+$	3.004	—	-3.57 ± 0.03	$\frac{7}{2}^+$	$\frac{9}{2}^+$	<1.8	58 ± 0.8

[a]Reference [33].
[b]Reference [34].
[c]Reference [35].
[d]Reference [19].
[e]104 ± 4 [36].
[f]Reference [34].

sions is given in Table II. For ^{23}Na, it can be said that the properties of the g.s. and $\frac{5}{2}^+$ and $\frac{7}{2}^+$ states are well described in the rotational model with band spin $K=\frac{3}{2}$. The structure of the ^{27}Al nucleus is much more intriguing. Tests of the rotational model in terms of the measured quadrupole moment and $B(E2)$ values of low-lying states have been done for ^{27}Al [16–18]. A simple prediction of $B(E2)$ values based on a recent experimental g.s. quadrupole moment [19] in the strong-coupled rotational model with the band spin $K=\frac{5}{2}$ is shown in Table II. The strongest state coupled to the g.s. of ^{27}Al is the $\frac{7}{2}^+$ state at $E_{\text{ex}}=2.211$ MeV while a slightly weaker coupling to the low-lying states of $\frac{1}{2}^+$ ($E_{\text{ex}}=0.844$ MeV) and $\frac{3}{2}^+$ ($E_{\text{ex}}=1.014$ MeV) also exists [20]. Since a detailed interpretation of the observed spectroscopic quantities requires more elaborate models such as band mixing [18,21], coupling of rotation and vibration [17], strong interaction between different Nilsson orbits [22], or a weak-coupling model [23], a simple rotational model is also taken for the ^{27}Al nucleus to reduce the uncertainty of the parameters involved. Hence only the coupling between the g.s. and $\frac{7}{2}^+$ and $\frac{9}{2}^+$ states is included in the calculation, while there has been a consideration of the $\frac{9}{2}^+$ state at 3.004 MeV as the band head of a $K=\frac{9}{2}$ band [17].

The nuclear deformation length used in the coupled-channel calculation is given by $\delta_2=1.57$ fm [11] for ^{23}Na and $\delta_2=1.11$ fm for ^{27}Al, obtained by using the intrinsic-charge quadrupole moment of ^{27}Al g.s. rotational band, $Q_0=39.26$ e fm^2, and by assuming the nuclear deformation length is the same as the Coulomb deformation length. The reduced matrix elements $M(E2)$ are obtained according to the convention in FRESCO by using the rotational model description for ^{23}Na and ^{27}Al. In channel couplings, up to two or three states including the g.s. for ^{23}Na and ^{27}Al nuclei, respectively, are considered. The coupling schemes are summarized in Table III, where the first and second roman numerals denote the number of coupled states of the projectile ^{23}Na and of the target ^{27}Al, respectively. Owing to the long-ranged Coulomb coupling, the radial integration of the wave function has been performed to a maximum radius of 25 fm and a further extension using the coupled Coulomb functions to an asymptotic radius of 60 fm has been done for a maximum of 450 partial waves to give reliable results for $\theta_{\text{c.m.}}>3°$.

III. EXPERIMENT

The experiment was performed using a ^{23}Na beam from the polarized heavy-ion source [24] at the Nuclear Structure Facility at Daresbury Laboratory in the UK. Polarization of the beam was achieved using rf transitions between the 2-8 and 4-6 hyperfine atomic levels [25] in a magnetic field, theoretically leading to equal magnitude positive and negative t_{20} polarizations, respectively. The equality of the t_{20} polarizations for the two transitions was verified by comparison with an unpolarized beam. Odd-rank polarizations are equal in each case and so may be eliminated by use of the two polarized beam states and an unpolarized state. The polarization states were switched every few seconds after a specified integrated beam current was measured, to minimize

TABLE III. The coupling schemes used in the calculation for projectile and target nuclei. (Reorientation is always included.)

Notation	Coupled states ^{23}Na	^{27}Al
I-I	g.s.($3/2^+$)	g.s.($5/2^+$)
II-I	g.s.($3/2^+$) and $5/2^+$	g.s.($5/2^+$)
I-II	g.s.($3/2^+$)	g.s.($5/2^+$) and $7/2^+$
I-III	g.s.($3/2^+$)	g.s.($5/2^+$), $7/2^+$ and $9/2^+$

systematic errors due to beam drift or polarization fluctuations. A Wien filter was used to orient the polarization symmetry axis along the beam direction on the target, for the T_{20} measurements and normal to the scattering plane for the ${}^{T}T_{20}$ measurements. The polarized $^{23}Na^{-}$ ions were accelerated to the terminal of a tandem Van de Graaff accelerator, charge stripped by a carbon foil, and then further accelerated. $^{23}Na^{9+}$ ions after stripping were selected because the yield was greater than for $^{23}Na^{11+}$ and a closed two-electron atomic shell is known to suffer much less depolarization of the beam in the stripper foil [26]. The 150-MeV accelerated beam was incident on an ^{27}Al target of thickness 350 $\mu g\,cm^{-2}$ in the target chamber of a QMG/2 magnetic spectrometer.

The beam was collected after the target in a polarimeter and beam-stop assembly which was especially built to be small enough to allow measurements to be made with the spectrometer at scattering angles as small as 4° in the laboratory frame. The beam polarization was determined using the $^{1}H(^{23}Na,\alpha)^{20}Ne$ polarimeter reaction for which $T_{20}=-1$ and ${}^{T}T_{20}=0.5$ at 0°, due to angular momentum considerations [27]. The target for this reaction was a $1-mg\,cm^{-2}$ titanium foil into which hydrogen had been absorbed. The α particles were detected and identified in a ΔE-E silicon detector telescope at 0°, with angular acceptance 3°, after passing through a 50-μm tantalum beam stop. The measured beam polarization was typically $t_{20}=0.1$.

The ^{23}Na nuclei scattered from the ^{27}Al target entered the QMG/2 magnetic spectrometer via an aperture of solid angle 10 msr and angular acceptance 6°. They were detected using a gas detector [28] in the focal plane of the spectrometer. Use of the spectrometer allowed the elastic scattering to be resolved from the inelastic scattering, leading to the 0.44-MeV first-excited state in ^{23}Na. Selection of elastic scattering events and determination of the scattering angle were achieved using energy and position signals available from the focal-plane detector. Data were transmitted from analog-to-digital converters to a computer and recorded event by event on tape.

T_{20} and ${}^{T}T_{20}$ data were obtained for a range of scattering angles from 4° to 15.2° and 10°, respectively, in the laboratory frame.

IV. RESULTS

The analyzing powers obtained are shown in Fig. 1. The error bars shown in the analyzing power data are statistical. Systematic errors in yields may arise from target-thickness variation and movement of the beam spot on target, with associated acceptance variations into the magnetic spectrometer and focal-plane detector. However, analyzing powers are extracted from ratios of yields for which all these factors are identical and therefore cancel, resulting in negligible systematic errors in the analyzing powers. The magnetic spectrometer can be reproducably accurately positioned, so systematic errors on the angle are negligible, as evidenced by the extremely close agreement of the middle two T_{20} data points near 18° in Fig. 1. The angular resolution is indicated by the angle error bars shown.

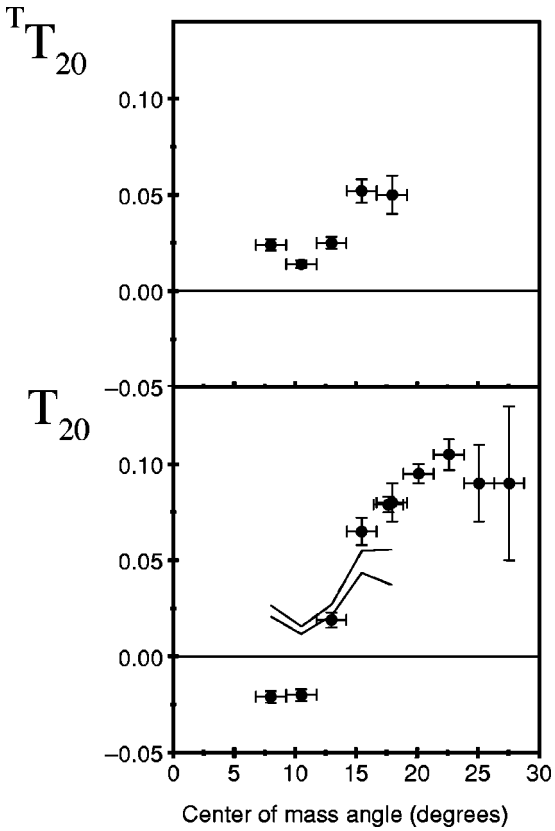

FIG. 1. Analyzing powers for elastic scattering of 150 MeV ^{23}Na from ^{27}Al. The curves show the shape-effect prediction for T_{20} calculated from the ${}^{T}T_{20}$ data.

The shape-effect relation given in Eq. (1) was used to calculate T_{20} from the ${}^{T}T_{20}$ data. The results of this calculation for the limits given by the ${}^{T}T_{20}$ analyzing power error bars are shown with the T_{20} data in Fig. 1. The data exhibit a clear deviation from the shape-effect relation, especially at forward angles. In particular the forward-angle T_{20} data are of negative sign while the ${}^{T}T_{20}$ data and shape-effect prediction are positive. The results of coupled-channel calculations are shown in Figs. 2 and 3. By fixing the potential, the effect of channel coupling is shown for the calculation of coupled projectile or target states. As more states are coupled, the oscillating behavior at large angles is smoothed out [29]. Reproduction of the ${}^{T}T_{20}$ data is reasonable, but much better for the T_{20} data as more target states are coupled into the calculation. Hence the best results are obtained for the coupling scheme of g.s. reorientation for ^{23}Na and the three coupled states ($5/2^{+}$ g.s.,$7/2^{+}$,$9/2^{+}$) of ^{27}Al, giving a good reproduction especially for the T_{20} data at forward angles.

To check the deviation from tidal symmetry and the shape-effect relation, a simple comparison of the ratio $T_{20}/{}^{T}T_{20}$ is shown in Fig. 4 for the experimental data, the shape-effect relation, and the coupled-channel calculations. For the angular range covered by the data the ratio of the analyzing powers as predicted by the shape-effect relation is close to 1. At large angles above the Coulomb rainbow angle

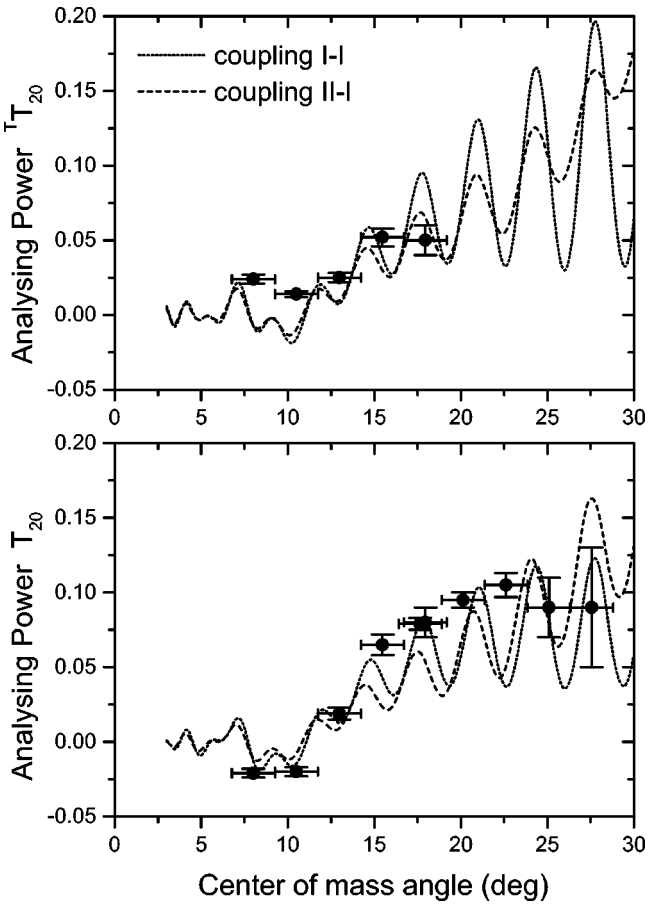

FIG. 2. Results of a coupled-channel calculation by coupling more states of the ^{23}Na projectile. The coupling scheme is shown in Table III.

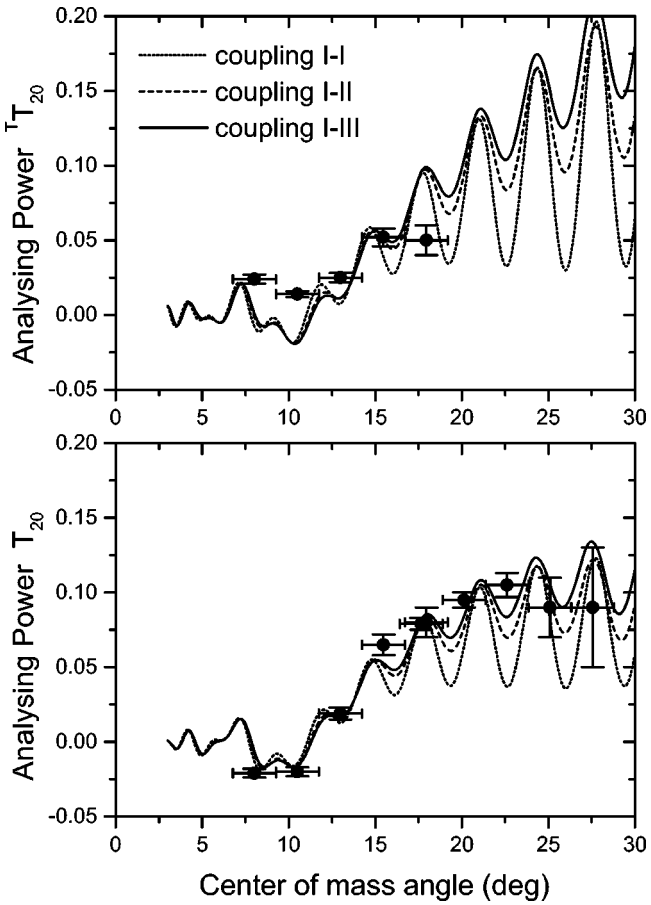

FIG. 3. Results of a coupled-channel calculation by coupling more states of the ^{27}Al target. The coupling scheme is shown in Table III.

of 11°, little deviation from the prediction of the shape-effect relation is seen, which is also supported by the coupled-channel calculations. The clear deviation of the data and coupled-channel calculations from the shape-effect prediction, however, is highlighted at forward angles, where the Coulomb excitation is dominant. The discontinuities in the ratio given by the coupled-channel calculation correspond to the angles of zero $^{T}T_{20}$ value. The deviation of the data and calculation from the shape-effect relation is indicative of tidal symmetry breaking at forward angles. This feature contrasts with satisfactory shape-effect relations for elastic scattering for ^{7}Li+^{120}Sn at 44 MeV [7] and ^{7}Li+^{54}Fe at 70 MeV [8], even though these systems have larger isocentrifugal parameters than that of the present scattering system. Here the values of isocentrifugal parameter are based on the estimation by Ott *et al.* [5], which has considered the nuclear coupling only. When the isocentrifugal parameter is considered for the long-range Coulomb coupling, its value is dependent on the scattering angle and approaches 2/3 as the scattering angle approaches zero in the case of elastic scattering [30]. Hence the present study apparently supports the previous conclusion [30] that tidal symmetry deteriorates at small scattering angles. Since the rank-2 analyzing powers are mostly close to zero or unmeasured in the forward angular region of Coulomb dominance in the previous measurements [6,7,9–11], it remains, however, to be understood quantitively if the present deviation from tidal symmetry at forward angles can be explained by the long-range nature of the Coulomb coupling. In addition it is possible, particularly at small angles, that as well as scattering from the near side

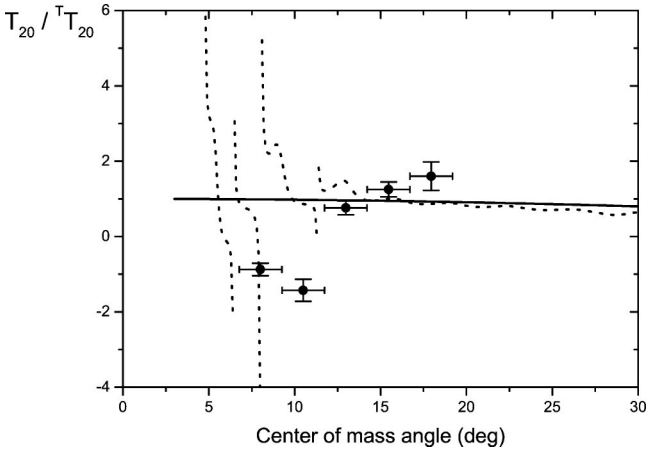

FIG. 4. Experimental ratio of analyzing powers compared with the shape-effect prediction (solid curve) and the coupled-channel calculation (dashed curve) obtained using coupling scheme I-III in Table III.

of the target nucleus, the same angle of scatter can be achieved by a partial orbit of the projectile around the far side of the target nucleus. This far-side contribution is likely to be a very small fraction of the yield, but could potentially have a more significant effect on the analyzing powers [31].

V. CONCLUSIONS

The analyzing powers T_{20} and ${}^{T}T_{20}$ have been measured for elastic scattering of 150 MeV ^{23}Na from a ^{27}Al target. This system has a small isocentrifugal parameter so tidal symmetry would ordinarily be expected to hold. However, a marked deviation from tidal symmetry is observed at forward angles which may arise due to target deformation, a long-range Coulomb coupling to excited states, or the contribution of the far-side amplitude. In previous experimental studies [6–11], the small isocentrifugal parameters led to a validity of tidal symmetry and shape-effect relation in the elastic channel even though the breaking of tidal symmetry to some degree was observed for the inelastic channels. The current study however, shows the breaking of tidal symmetry and shape-effect relation even for the elastic channel in the forward-angular range.

The results of this investigation indicate that further elastic scattering measurements for other systems involving deformed target nuclei are highly desirable, in order to determine whether a similar deviation from tidal symmetry is indeed observed. While the measurement of two rank-2 analyzing powers is the minimum requirement for determining deviation from tidal symmetry, ideally all three rank-2 analyzing powers would provide a more complete data set. In addition, measurement of odd-rank analyzing powers would also be of interest because these are zero if tidal symmetry holds. It would be interesting to observe how any tidal symmetry breaking is manifested in the odd-rank analyzing powers.

The ^{27}Al target nucleus used for the current measurements, as well as being deformed, also has a nonzero spin, with a $5/2^{+}$ ground state. The nuclear spin is not expected to affect tidal symmetry [32]. However, it would be good to confirm this by performing elastic-scattering measurements for deformed target nuclei with both zero and nonzero spins.

ACKNOWLEDGMENTS

We would like to thank the Engineering and Physical Sciences Research Council for funding some of this project. K.L. acknowledges additional financial support from Micron Semiconductor Ltd.

[1] J. Gomez-Camacho and R.C. Johnson, J. Phys. G **12**, L235 (1986).
[2] J. Gomez-Camacho and R.C. Johnson, J. Phys. G **14**, 609 (1988).
[3] G. Tungate and D. Fick, in *Lecture Notes in Physics*, edited by H.V. Geramb (Springer-Verlag, Berlin, 1979), Vol. 89.
[4] *Madison Convention, Proceedings of the 3rd International Symposium on Polarization Phenomena in Nuclear Reactions*, edited by H.H. Barschall and W. Haeberli (University of Wisconsin Press, Madison, 1971).
[5] W. Ott, R. Butsch, H. Jänsch, G. Tungate, E. Steffens, K. Becker, K. Blatt, H. Leucker, D. Fick, J. Gomez-Camacho, and R.C. Johnson, J. Phys. G **14**, L7 (1988).
[6] Z. Moroz, P. Zupranski, R. Böttger, P. Egelhof, K.H. Möbius, G. Tungate, E. Steffens, W. Dreves, I. Koenig, and D. Fick, Nucl. Phys. **A381**, 294 (1982).
[7] G. Tungate, D. Krämer, R. Butsch, O. Karban, K.H. Möbius, W. Ott, P. Paul, A. Weller, E. Steffens, K. Becker, K. Blatt, D. Fick, B. Heck, H. Jänsch, H. Leucker, K. Rusek, I.M. Turkiewicz, and Z. Moroz, J. Phys. G **12**, 1001 (1986).
[8] G. Kuburas, O. Karban, C.O. Blyth, H.D. Choi, S.J. Hall, S. Roman, G. Tungate, I.M. Turkiewicz, and N.J. Davis, Nucl. Phys. **A542**, 479 (1992).
[9] O. Karban, C.O. Blyth, H.D. Choi, K.A. Connell, S.E. Darden, N.J. Davis, J.B.A. England, S.J. Hall, S. Roman, A.C. Shotter, and G. Tungate, J. Phys. G **14**, L261 (1988).
[10] H. Leucker, K. Becker, K. Blatt, W. Korsch, W. Luck, H. Reich, H.G. Völk, D. Fick, R. Butsch, H. Jänsch, and Z. Moroz, Phys. Rev. Lett. **62**, 2241 (1989).
[11] H.D. Choi, C.O. Blyth, S.J. Hall, O. Karban, G. Kuburas, S. Roman, G. Tungate, N.J. Davis, A.C. Shotter, K.A. Connell, and S.E. Darden, Nucl. Phys. **A529**, 190 (1991).
[12] W.E. Frahn, Phys. Rev. Lett. **26**, 568 (1971).
[13] N. Rowley, Nucl. Phys. **A219**, 93 (1974).
[14] I.J. Thompson, Comput. Phys. Rep. **7**, 167 (1988).
[15] J.D. Garrett, H.E. Wegner, T.M. Cormier, E.R. Cosman, Ole Hansen, and A.J. Lazzarini, Phys. Rev. C **12**, 489 (1975).
[16] R. Weber, B. Jeckelmann, J. Kern, U. Kiebele, B. Aas, W. Beer, I. Beltrami, K. Bos, G. de Chambrier, P.F.A. Goudsmit, H.J. Leisi, W. Ruckstuhl, G. Strassner, and A. Vacchi, Nucl. Phys. **A377**, 361 (1982).
[17] H. Röpke, V. Glattes, and G. Hammel, Nucl. Phys. **A156**, 477 (1970).
[18] D. Dehnhard, Phys. Lett. **38B**, 389 (1972).
[19] Dage Sundholm and Jeppe Olsen, Phys. Rev. Lett. **68**, 927 (1992).
[20] P.M. Endt and C. van der Leun, Nucl. Phys. **A310**, 1 (1978).
[21] C.L. Lin and F.J. Kline, Tohoku University Laboratory of Nuclear Science Research Report, Vol. 10, supplement, 1977 (unpublished).
[22] H.G. Price, P.J. Twin, A.N. James, and J.F. Sharpey-Schafer, J. Phys. A **7**, 1151 (1974).
[23] R.S. Hicks, A. Hotta, J.B. Flanz, and H. de Vries, Phys. Rev. C **21**, 2177 (1980).
[24] O. Karban, W.C. Hardy, K.A. Connell, S.E. Darden, C.O. Blyth, H.D. Choi, S.J. Hall, S. Roman, and G. Tungate, Nucl. Instrum. Methods Phys. Res. A **274**, 4 (1989).
[25] E. Steffens, W. Dreves, P. Egelhof, D. Kasen, W. Weiss, P.

Zupranski, and D. Fick, Rev. Phys. Appl. **12**, 1567 (1977).
[26] H. Jänsch, K. Becker, K. Blatt, H. Leucker, D. Fick, R. Butsch, B. Heck, D. Krämer, K.H. Möbius, W. Ott, P. Paul, R. Suntz, G. Tungate, I.M. Turkiewicz, A. Weller, and E. Steffens, Nucl. Instrum. Methods Phys. Res. A **254**, 7 (1987).
[27] P. Zupranski, W. Dreves, P. Egelhof, E. Steffens, D. Fick, and F. Rösel, Nucl. Instrum. Methods **167**, 193 (1979).
[28] R.A. Cunningham, N.E. Sanderson, W.N.J. Snodgrass, D.W. Banes, S.D. Hoath, and J.N. Mo, Nucl. Instrum. Methods Phys. Res. A **234**, 67 (1985).
[29] G.R. Satchler, *Direct Nuclear Reactions* (Clarendon, Oxford, 1983), p. 496.
[30] R.C. Johnson, in *Proceedings on Heavy Ion Collisions near the Coulomb Barrier*, edited by M. A. Nagarajan (IOP Publishing, Bristol, 1990).
[31] J. Gomez-Camacho, in *Proceedings of Workshop on Heavy Ion Collisions near the Coulomb Barrier* [30].
[32] R.C. Johnson (private communication).
[33] B. Jeckelmann, W. Beer, I. Beltrami, F.W.N. de Boer, G. de Chambrier, P.F.A. Goudsmit, J. Kern, H.J. Leisi, W. Ruckstuhl, and A. Vacchi, Nucl. Phys. **A408**, 495 (1983).
[34] D. Schwalm, E.K. Warburton, and J.W. Olness, Nucl. Phys. **A293**, 425 (1977).
[35] M.J.A. de Voigt, P.W.M. Glaudemans, J. de Boer, and B.H. Wildenthal, Nucl. Phys. **A186**, 365 (1972).
[36] R.P. Singhal, A. Johnston, W.A. Gillespie, and E.W. Lees, Nucl. Phys. **A279**, 29 (1977).